Modeling demand response of Charge Point Operators to consider flexibility in grid planning

António Maria Jerónimo
INESC ID / Instituto Superior Técnico
Lisbon, Portugal
antonio.jeronimo@tecnico.ulisboa.pt

Pedro Carvalho
INESC ID / Instituto Superior Técnico
Lisbon, Portugal
pcarvalho@tecnico.ulisboa.pt

Célia Jesus
INESC ID / Instituto Superior Técnico
Lisbon, Portugal
celiaj@tecnico.ulisboa.pt

Luiz Dias
EDP NEW
Lisbon, Portugal
luiz.dias@edp.pt

Luís Marcelino Ferreira
INESC ID / Instituto Superior Técnico
Lisbon, Portugal
lmf@tecnico.ulisboa.pt

Hugo Morais
INESC ID / Instituto Superior Técnico
Lisbon, Portugal
hugo.morais@tecnico.ulisboa.pt

***Abstract*—Electric Vehicles (EVs) are creating new challenges to power system planning and operation such as grid overloads and voltage deviations, particularly at the distribution system level, while simultaneously offering new opportunities in congestion management through their ability to provide flexibility. Traditional planning methodologies consider the trade-off of investment costs against improved system reliability and energy efficiency. However, to embed EV flexibility into grid planning, models that estimate the flexibility of Charging Point Operators (CPOs) managing EV charging stations are necessary. For that, CPOs need to be characterized, allowing estimation of their flexibility, in particular, their ability to reduce grid overloads (congestions) and voltage deviations, as well as their operational costs when providing such flexibility. In this paper, a new flexibility model for CPO flexibility is proposed, which characterizes CPOs based on their charging and occupancy rates. The model is then embedded into the grid planning problem by defining a new flexibility cost function. An illustrative example is presented to show how the proposed model is embedded into optimal planning. The obtained results show an example where the best investment is an hybrid solution between traditional reinforcement investment and the use of flexibility.**

***Index Terms*—Charge point operator, distribution system planning, electric vehicles, load charging schedule, particle hopping models.**

NOMENCLATURE

R	Reliability cost function.
$R^{'}$	Modified reliability cost function.
S	Energy losses cost function.
I	Investment cost function.
F	Flexibility cost function.
C	Charging rate.
O	Occupancy rate.
N	Number of EV charger outlets of a CPO.
P	Chargers power of a CPO.
d_c	Charging density.
d_o	Occupancy density.
ENS_x	Energy not served in branch x
$\mathrm{ENS}_x^{'}$	Reduced energy not served in branch x due to load being shifted by flexibility

This research work was funded by European Union's Horizon Europe R&I programme under grant agreement no. 101056765. Views and opinions expressed in this document are however those of the authors only and do not necessarily reflect those of the European Union or the European Climate, Infrastructure and Environment Executive Agency (CINEA). Neither the European Union nor the grating authority can be held responsible for them. This work was also funded by the Portuguese Foundation for Science and Technology (FCT) under UIDB/50021/2020.

I. INTRODUCTION

A. Motivation and Background

WITH the increased uptake in Electric Vehicles (EVs), distribution grids must be correctly planned so that overload and voltage impacts are mitigated while avoiding increased active power losses and decreased quality of service [1]. To mitigate these impacts, Distribution System Operators (DSOs) will have to reinforce the grid infrastructure and/or adopt new planning strategies considering the use of flexibility as an alternative to traditional grid reinforcement [2], [3].

Although EVs can bring additional challenges to distribution grid planning, charging point operators (CPOs) may offer power demand flexibility [4], the potential of which can be exploited through smart charging [5]. Under flexibility contracts, EVs can be seen as temporary capacity providers, enabled for a price, allowing deferring of grid reinforcement decisions [1].

In the business-as-usual planning, congestions are translated into energy not supplied (ENS). Often, the regulators set an economical value for kWh of the ENS so that the reliability costs, R, can be traded against the energy loss costs, S and the investment costs, I [6]. Based on such an economic value, the distribution grid planning tools of today search for optimal planning solutions by minimizing the corresponding total costs of R, S, and I. Such cost functions must be evaluated on a given planning horizon.

To incorporate flexibility into the distribution grid planning problem, future planning tools should consider a new cost function for the flexibility of power demand, F. To define such a function, a model must be developed for EV flexibility pricing and capabilities. Such a model should, on one hand,

be capable of representing load reduction capabilities of CPO, their limitations, and associated costs, and, on the other hand, be simple enough not to overburden the decision-making process behind optimal planning.

B. Relevant Literature

This paper proposes a novel method, inspired by the work presented in [7] to model the flexibility of EVs and mainly of CPOs to be represented in the planning problem to be used by DSOs. In [7] the ramping limitations of direct controlled load-shifting response dynamics were studied. To accomplish this, the authors have used a particle hopping model, introducing the concepts of load density and shifting velocity to quantify the ramping capabilities of ideal load-shifting (V1G) responses. These concepts will be explored again later on, as the proposed model relies on such concepts.

Following [7], incentive-based load-shifting dynamics were studied in [8] to simulate aggregate responses and analyze their predictability under time-varying prices. Vehicle-to-grid (V2G) capabilities were later added in [9], where it was concluded that V2G residually increased the responsive capabilities of aggregators, *i.e.*, the number of V2G decisions were found to be minimal when compared to V1G decisions. However, if the response is controlled indirectly through prices or incentives, the evidence demonstrated that V2G might make control easier, decreasing response mismatches and consequently decreasing the cost for the aggregator.

C. Contributions and Organization

The model used to evaluate the ramping limitations in load-following capabilities in [7]–[9] assumed that EV charging stations were always fully occupied, meaning that the EV chargers outlets were always connected to EVs. This, in turn, resulted in maximum flexibility assessment. We evolve such model by introducing the concepts of occupancy density, thus dropping the mentioned assumption.

This paper is organized as follows. In Section II, EV CPO flexibility for congestion management is modeled and evaluated. In Section III, we define and include the new flexibility cost function into the optimal planning problem. In Section IV, an illustrative example is presented to show how the proposed model may be embedded into optimal planning. In Section V, we conclude the paper.

II. Modeling CPO flexibility for congestion management

A. Characterization of CPOs

The proposed model characterizes the load reduction capabilities of CPOs using four parameters: the charging rate, C, the occupancy rate, O, the number of EV charging outlets, N, and respective nominal power, P. These parameters are defined by the CPO and communicated to the DSO, in order to be included in the planning problem.

Both the charging and occupancy rates are given as a percentage. The charging rate refers to the percentage of EV charger outlets that are actively charging an EV, whereas the occupancy rate refers to the percentage of EV charger outlets that are occupied (either charging an EV or idling with the EV connected). Each outlet can only be connected to a single EV. The proposed model considers that EV charger outlets operate always at nominal power.

Figure 1 represents an example of the charging and occupancy rates of a CPO representative of workplace charging, obtained through the analysis of a 52 EV parking lot located in the *NASA Jet Propulsion Laboratory* using the *Adaptive Charging Network* dataset [10]. The time resolution is set for 15 minutes, as this is the normal time resolution used by DSOs in the planning phase, allowing for an adequate representation of the use of charging stations [10].

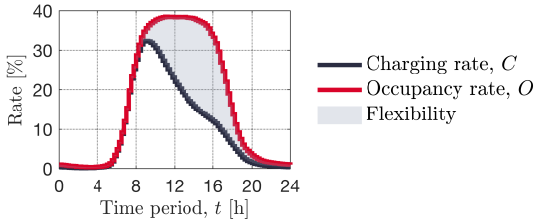

Fig. 1. An example of a charging and occupancy rates of work charging station operators.

B. Modeling CPO Shifting Flexibility

We consider the use of particle-hopping models to simulate a variety of dynamic processes of the charging of EVs managed by CPOs. These models have been used to simulate a variety of dynamic processes, including traffic flow [11], [12]. Here, we use a particle hopping model to assess the shifting flexibility of CPOs. Shifting flexibility is represented as a particle hopping process on EV charging schedules, with each charger outlet charging schedule represented as a one-dimensional lattice of cells, where each cell represents a time period.

The EV charging schedules are modeled using a non-homogeneous discrete-time Markov chain. Let $\mathbf{\Omega} = \{0, 1, 2\}$ be the set of possible states. State 0 refers to a situation when the charger outlet is empty (no EV is connected), state 1 when the charger outlet is actively charging (EV is connected and charging), and state 2 when the charger outlet is idle (EV is connected but not charging).

Charge schedules span 24 hours ($T = 24\,\mathrm{h}$) using a time resolution of $\tau = 15$ min, resulting in 96 representative periods. Thus, they can be represented as a sequence of random variables X_k. X_k can assume any value of $\mathbf{\Omega}$ at each time period k. To parameterize the non-homogeneous Markov process, it is necessary to define the state probabilities of all states, Π, as well as the Markov transition matrix, $\mathbf{P} = [p^{ij}]$, for each time period k. Hereafter, the subscript k is used for the variables Π and $\mathbf{P}$ to denote time periods.

The state probabilities for each time period are set by the charging and occupancy rates. Defining the row vector Π_k as

$$\begin{aligned}\Pi_k &= \begin{bmatrix}\Pi_k^0 & \Pi_k^1 & \Pi_k^2\end{bmatrix} \\ &= \begin{bmatrix}\mathbb{P}(X_k = 0) & \mathbb{P}(X_k = 1) & \mathbb{P}(X_k = 2)\end{bmatrix},\end{aligned} \tag{1}$$

it follows that Π_k^0 corresponds to the complement of the occupancy rate, Π_k^1 to the charging rate, and Π_k^2 to the difference between the occupancy and the charging rate. Mathematically, $\Pi_k^0 = 1 - O_k$, $\Pi_k^1 = C_k$ and $\Pi_k^2 = O_k - C_k$.

Since $\mathbf{\Omega}$ is of size 3, then the Markov transition matrices will be 3×3 squared matrices with each entry, p_k^{ij}, representing the probability of being at state i at time period k and transitioning to state j in the next time period $k+1$.

The parameters given by the CPO do not allow the computation of the Markov transition probabilities. Thus, they have to be estimated. An algorithm for the estimation of the Markov transition probabilities is used, but it is not presented, as it is out of the scope of this paper. The estimation of the Markov transition probabilities allows the non-homogeneous Markov process to be fully parameterized.

Consequently, it is possible to generate a sequence of states corresponding to the charging schedule of each EV charger outlet contained in the charging station. By performing N Markov chain simulations, the charging schedules are set for all the outlets. By stacking the N charging schedules, a two-dimensional lattice is obtained. In this lattice, the *x-axis* dimension refers to the time stamp dimension of the charging schedules and the *y-axis* dimension refers to the cardinality of the EV charger outlet. Figure 2 depicts an example of the charging schedules of 10 EV charger outlets from 06:00 to 20:00, represented in a lattice.

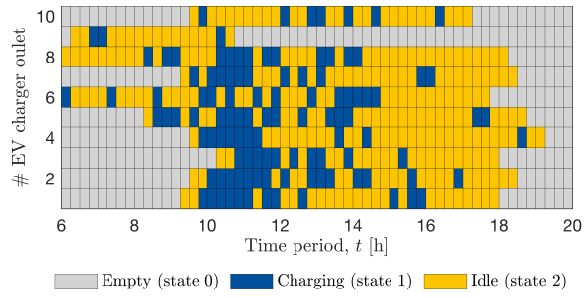

Fig. 2. Example of a lattice representing the original charging schedules, on a 15 min basis, of 10 EV charger outlets.

Shifting flexibility is represented in lattices by the idle particles ahead of each charging particle. By deciding which charging particles are to be shifted ahead into an idle position, it is possible to regulate the power output of the flexibility resource. Consequently, the configuration of the lattice in time period $k+1$ is determined in time period k. The process is, therefore, dynamic because the charging particles available to be shifted ahead in a given time period k and their flexibility depends on the number of charging particles that one decided to shift ahead in time $k-1$.

Since flexibility is defined as a 'controlled power adjustment sustained for a required duration' [1], the correct assessment of the ability to reduce the power output of a CPO in response to external calls for load reduction becomes necessary to evaluate the flexibility capabilities within each CPO. In the following subsection, we address this issue.

C. Flexibility Evaluation of CPOs

Let the EV charger outlets be identified by $n = 1, \ldots, N$ and L be the aggregate normalized demand of the EV charging station, such that

$$L(k) = \sum_{n=1}^{N} x_n(k) \quad \forall\, k \in \mathcal{K} \tag{2}$$

where $\mathcal{K} = \{1, ..., T/\tau\}$ and $x_n(k) \in \{0, 1\}$ corresponds to the load demand of the n$^{\text{th}}$ charger outlet in the time period k ($x_n = 0$ if the charger outlet is either empty or idle and $x_n = 1$ if the charger outlet is charging). Additionally, let L^* be the normalized target demand set for the EV charging station in time period k.

Consider a peak shaving service requested by the DSO. Let the necessary reduction in aggregate load to yield target L^* be denoted by ΔL^*, such that

$$\Delta L^*(k) = L(k) - L^*(k). \tag{3}$$

Aggregate load reductions are obtained by controlling the number of charging particle shifts, according to

$$v(k) = \sum_{n=1}^{N} v_n(k) \quad \forall\, k \in \mathcal{K} \tag{4}$$

where $v_n(k)$ is unitary if a charging particle is shifted in time period k and zero otherwise. As $v(k)$ refers to the number of particles shifted in the time period k, then v can be thought of as a shifting velocity. Thus, changes in aggregate load are due to changes in shifting velocity [7], such that

$$\Delta L^*(k) \approx v(k) - v(k-1). \tag{5}$$

Figure 3 depicts an arbitrary peak to shave with duration $\Delta T = T_2 - T_1$. Let ΔT denote congestion time. During the time interval T_1 to T_2, $\Delta L^* > 0$ and thus shifting velocity increases, reaching a maximum at T_2. The time evolution of the shifting velocity is given by

$$v(k) = \sum_{k} \Delta L^*(k) \quad \forall k \in \{T_1, T_1 + \Delta T\}. \tag{6}$$

Letting v^* be the maximum shifting velocity, it follows that v^* corresponds to the area of the peak to be shaved,

$$v^* = v(T_2) = \frac{\Delta T \Delta L}{2}. \tag{7}$$

However, in each time period k during congestion time, v is limited. Let $\mathcal{V}_{\text{lim}}$ denote this limit. It follows that if

$$v(k) < \mathcal{V}_{\text{lim}}(k), \tag{8}$$

then the resource is flexible enough to shave such peak. $\mathcal{V}_{\text{lim}}$ can be thought of as a ceiling for v. Recalling that charging particles can only be shifted forward into idle positions, then $\mathcal{V}_{\text{lim}}$ is proportional to the probability of having idle positions ahead of a charging particle. Such a probability changes over the congestion time as the charging particles are shifted ahead.

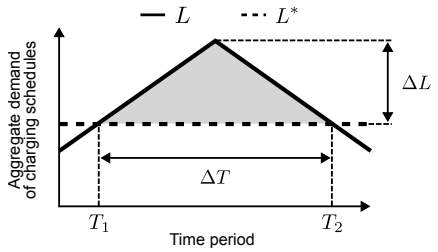

Fig. 3. Integration of the peak to shave with magnitude ΔL and duration ΔT to compute maximum shifting velocity, v^*.

Although mathematically correct, assessing such probability is a very cumbersome process due to shifting dynamics.

To overcome this challenge we consider the lattice to be homogeneous during congestion time. This allows the introduction of two new concepts: the charging density d_c, and the occupancy density d_o. Charging density is defined as the average of the charging rate during congestion time;

$$d_c = \frac{1}{\Delta T} \sum_{k=T_1}^{T_2} C(k), \tag{9}$$

and the occupancy density as the average of the occupancy rate during congestion time,

$$d_o = \frac{1}{\Delta T} \sum_{k=T_1}^{T_2} O(k). \tag{10}$$

The difference between d_o and d_c yields the average probability of finding an idle position at each time period during congestion time. We argue that such probability can be used to roughly evaluate the flexibility of a resource. Letting $\mathcal{V}^*_{\text{lim}}$ be the limit for maximum shifting velocity such that

$$\mathcal{V}^*_{\text{lim}} \approx (d_o - d_c)N, \tag{11}$$

then if

$$v^* \leq \mathcal{V}^*_{\text{lim}} \tag{12}$$

then the resource is considered to be flexibile enough to shave such peak.

Considering triangular peaks, as the one depicted in Fig. 3, Eq. (12) can be rewritten as

$$\Delta L \leq 2\frac{d_o - d_c}{\Delta T} N, \tag{13}$$

which encloses an important finding: the magnitude of the peak to shave is set by the charging and occupancy densities as well as the congestion time. For illustration purposes, consider Fig. 4 where the left column plots refer to a situation where peak shave is successful, whereas the right column plots depict one which is not.

III. Grid Planning with Flexibility

Assuming that several flexibility resources exist in the set of nodes $N_{\text{s-m}}$ delimited by the overloaded asset, s, and the faulted asset, m, then the maximum peak shaving magnitude that the DSO may procure to solve the overload in asset s due to a fault in asset m is given by

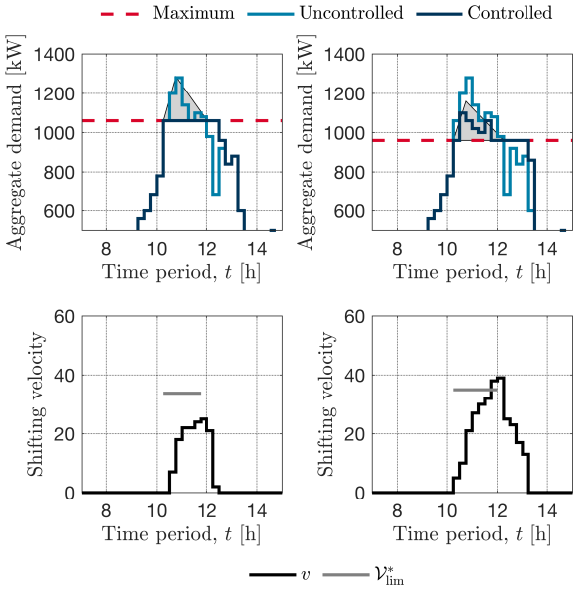

Fig. 4. Graphical representation of a situation where peak shave is successful (left column plots) and one where it is not (right column plots). The top row plots depict the maximum, uncontrolled and controlled aggregate demands and a shaded triangle with a width equal to the congestion time and magnitude given by Eq. (13). It is important to notice that in the successful shaving situation, the uncontrolled charging demand to be shaved is contained within the triangle. The bottom plots depict the time evolution of the shifting velocity. On the successful shaving situation, the maximum shifting velocity does not reach $\mathcal{V}^*_{\text{lim}}$.

$$D_m = \min \left\{ \sum_{\substack{g \in N_{\text{s-m}} \\ \pi_g < \gamma}} D_g, \quad \Delta L_m \right\} \tag{14}$$

where π_g corresponds to the marginal cost of the *negawatt-hour* of flexibility resource g, γ to the marginal cost of kWh of ENS, and ΔL_m to the load shed in the asset m, to guarantee security of supply. The term *negawatt-hour* refers to a unit of energy that is not used. Figure 5 depicts the nodes of the set $N_{\text{s-m}}$ for a fault on branch $m \equiv \text{d} - \text{f}$ and a post-fault configuration giving rise to an overload on branch $s \equiv \text{a} - \text{b}$.

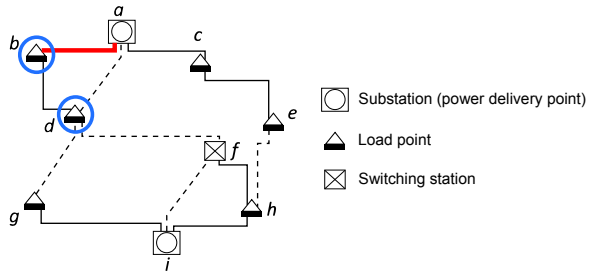

Fig. 5. Final stage of the service restoration process for a fault on branch $m \equiv$ d-f. In the post-fault configuration, the potential flexibility resources, $D_{\text{d-f}}$, likely to resolve the overload at branch $s \equiv \text{a} - \text{b}$, are identified in blue circles.

To quantify D_k, the charging and occupancy densities of the flexible resource must be known during the network

congestion period. Thus, according to Eq. (13), we have that

$$D_g = 2\frac{d_o - d_c}{\Delta T} N, \tag{15}$$

and using Eq. (14), the flexibility cost function is expressed as

$$F = \frac{1}{2} \sum_m \lambda_m \pi_m^* D_m \Delta T_m \tag{16}$$

where λ_m corresponds to the failure rate of the asset m and π_m^* to the clearing price for the purchased flexibility ΔL_m, assuming that the identified resources $\{D_g\}$ that compose D_m bid each its own price π_g. The value of π_m^* will depend upon the auction mechanism chosen to clear the supply $\{(D_g, \pi_g)\}$ against the procured demand ΔL_m (*e.g.*, pay-as-clear, pay-as-bid or other).

The optimal distribution grid planning problem considering flexibility is then formulated to include the flexibility cost function as derived in Eq. (16). The problem is formulated as a cost minimization problem whose objective can be expressed as:

$$\min\{R^{'} + S + I + F\} \tag{17}$$

where $R^{'}$ corresponds to a new reliability function, modified by considering that part of the expected load shed due to overloads and other congestions may be mitigated by enabling flexibility resources.

IV. Illustration of the Planning Methodology Considering CPOs Flexibility

A small scale 10 kV grid is presented in Figure 6. Consider the process of planning such grid for a target year $\mathcal{H}$. If a fault occurs in branch a − b, the fault is isolated and the grid is reconfigured to its post-fault configuration, as represented in Fig. 7. Due to expected load growth, branch f − e becomes overloaded during the post-fault configuration. This branch corresponds to an underground cable with a rated power of 6.75 MW. Additionally, let us consider that the change in the expected system ENS is solely given by part of the load downstream of the overloaded branch f − e (see Fig. 7) that must be shed in order to guarantee security of supply.

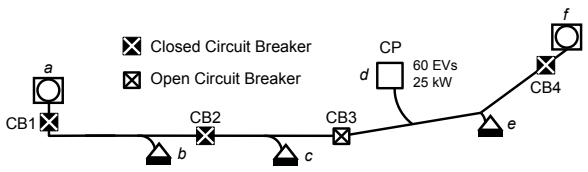

Fig. 6. A small scale 10 kV grid. The grid consists of two substations (busbars a and f), three inflexible load points (busbars b, c and e), a flexible resource corresponding to a charging station, managed by a CPO, with $N = 60$ EV charger outlets, each with a nominal power of $P = 25$ kW (busbar d) and 4 circuit breakers (CB1, CB2, CB3 and CB4).

Suppose that branch f − e is congested for one hour (from 11:00 to 12:00). Thus, $\Delta T_{\mathrm{a-b}} = 1\,\mathrm{h} = 4$ time periods (recall that $\tau = 15$ min). Moreover, the maximum overload is set to 10% of the rated power, *i.e.*, $\Delta L_{\mathrm{a-b}} = 675$ kW. The

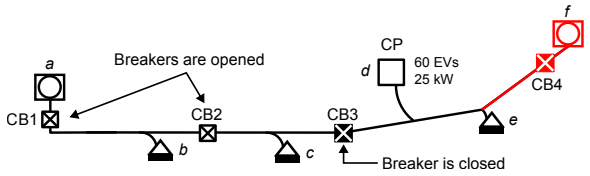

Fig. 7. Grid representation in its post-fault configuration for a fault in branch a − b, in which branch f − e becomes overloaded, due to load growth.

corresponding $\mathrm{ENS}_{\mathrm{f-e}}$ is depicted on the left plot in Fig. 8 where $\mathrm{ENS}_{\mathrm{f-e}}$ is approximated by the area of a triangle with a width equal to the congestion time and a magnitude equal to $\Delta L_{\mathrm{a-b}}$. Thus, we have $\mathrm{ENS}_{\mathrm{f-e}} = 337.5$ kWh.

To improve system reliability, energy efficiency, and quality of service, two grid planning strategies are proposed. The first one corresponds to the traditional grid reinforcement, in which the branch f − e is reinforced. The second corresponds to the deferment of grid reinforcement using flexibility resources. In the following paragraphs, both planning strategies are analyzed in detail.

Let us start by analyzing the traditional grid reinforcement strategy. Let the reinforcement of the branch f − e amount to a total investment cost, I_T, of 20 k€. The changes in the investment cost function, are simply given by the branch reinforcement investment annuity, such that

$$\Delta I = \frac{r(1+r)^H}{(1+r)^H - 1} I_T, \tag{18}$$

where r is the discount factor, set to 6.5%, and H corresponds to the asset's economic lifetime, set to 30 years. Consequently, Eq. (18) yields $\Delta I = 2.78$ k€/year.

Moreover, reinforcing such branch mitigates $\mathrm{ENS}_{\mathrm{f-e}}$, and therefore $\Delta\mathrm{ENS}_{\mathrm{f-e}} = -\mathrm{ENS}_{\mathrm{f-e}}$. The change in the reliability cost function is computed through

$$\Delta R = \lambda_{\mathrm{a-b}}\, \gamma\, \Delta\mathrm{ENS}_{\mathrm{f-e}}. \tag{19}$$

Considering a failure rate of branch a − b to be 0.5 ($\lambda_{\mathrm{a-b}} = 0.5\,\mathrm{year}^{-1}$, which means 1 fault every 2 years) and a marginal cost of ENS of $\gamma = 10$ €kWh^{-1}, the change in the reliability cost function yields $\Delta R = -1.69$ k€/year. Furthermore, a branch reinforcement reduces the losses in such branch. Thus, the change in the losses cost function is assumed to be $\Delta S = -1.20$ k€/year.

Let us now analyze the deferment of the grid reinforcement using flexible resources strategy. Recall that load point d is a flexible resource corresponding to a charging station operated by a CPO. Thus, such resource could be used to reduce or even mitigate the overload at branch f − e. The marginal cost of *negawatt-hour* of such a flexible resource is $\pi_d = 5$ €kWh^{-1}, less than the marginal cost of ENS. According to CPO characteristics, during congestion time, the charging and occupancy densities are set to 45% and 85%, respectively ($d_c = 0.45$, $d_o = 0.85$). Thus, according to Eq. (14), the maximum peak shaving magnitude yields $D_{\mathrm{a-b}} = 300$ kW.

The right plot of Fig. 8 depicts, in a shaded green triangle, with a width equal to the congestion time and a magnitude equal to $D_{\mathrm{a-b}}$, the load that can be shifted using flexibility resources. Thus, the reduced ENS in branch $\mathrm{f-e}$, $\mathrm{ENS}^{'}_{\mathrm{f-e}}$ is equal to the difference between the gray and green areas, *i.e.*, the blue area and therefore $\mathrm{ENS}^{'}_{\mathrm{f-e}} = 187.5\,\mathrm{kWh}$. Consequently, we have the following.

$$\Delta\mathrm{ENS}_{\mathrm{f-e}} = \mathrm{ENS}^{'}_{\mathrm{f-e}} - \mathrm{ENS}_{\mathrm{f-e}} = -150\,\mathrm{kWh}. \tag{20}$$

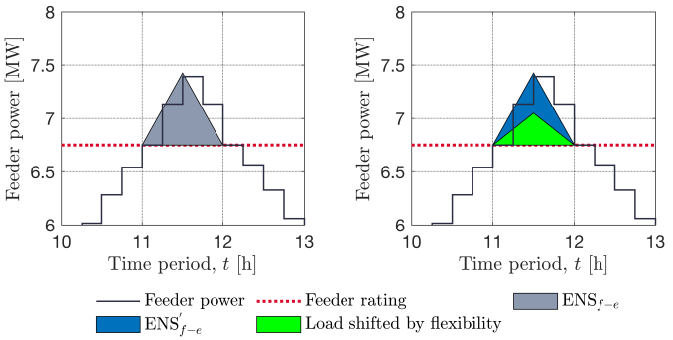

Fig. 8. Graphical representation of the ENS in branch $\mathrm{f-e}$ due to load growth (left plot) and the reduced ENS in branch $\mathrm{f-e}$ due to load being shifted by flexibility (right plot)

The change in the reliability cost function is again computed using Eq. (19), yielding $\Delta R = -0.75\,\mathrm{k€/year}$. The changes in both the energy losses and investment cost functions are zero since the investment is deferred.

Finally, the changes in the flexibility cost function are computed using

$$\Delta F = \frac{1}{2}\lambda_{\mathrm{a-b}}\,\pi^{*}_{\mathrm{a-b}}\,D_{\mathrm{a-b}}\,\Delta T_{\mathrm{a-b}}, \tag{21}$$

where the clearing price $\pi^{*}_{\mathrm{a-b}}$ is equal to π_{d}. Thus, we have $\Delta F = 0.38\,\mathrm{k€/year}$.

Table I sums up the results and presents the change in the total cost for both grid planning strategies. It can be concluded that for the target year $\mathcal{H}$, the use of the flexibility services strategy is a more cost-effective solution than the traditional one, which in turn allows for the deferral of the grid reinforcement investment to a later year than the target one.

TABLE I
COST ASSESSMENT OF BOTH GRID PLANNING STRATEGIES: TRADITIONAL GRID REINFORCEMENT AND GRID REINFORCEMENT DEFERMENT USING FLEXIBILITY RESOURCES

Change in cost function	**Traditional** [k€/year]	**Flexibility** [k€/year]
ΔR	-1.69	-0.75
ΔS	-1.20	0
ΔI	2.78	0
ΔF	—	0.38
Total	-0.11	-0.37

V. CONCLUSION

EVs introduce new opportunities for congestion management through their ability to provide flexibility. In this paper, a new model based on particle hopping is proposed to consider the flexibility of EVs, namely in assessing the load reduction capabilities of an EV charging station managed by a CPO. The model is then used to define a new flexibility cost function, which is embedded into the distribution grid planning problem, allowing the trade-off between reliability, energy losses, investment, and flexibility cost functions. The introduction of CPO flexibility in the planning problem can lead to hybrid optimal solutions, combining both flexibility and grid reinforcement strategies. An illustrative example was presented showing that the use of flexibility could be used to defer a grid reinforcement investment.

REFERENCES

[1] F. Gonzalez Venegas, M. Petit, and Y. Perez, "Active integration of electric vehicles into distribution grids: Barriers and frameworks for flexibility services," *Renewable and Sustainable Energy Reviews*, vol. 145, p. 111060, Jul. 2021.

[2] G. Celli, F. Pilo, G. Pisano, S. Ruggeri, and G. G. Soma, "Risk-oriented planning for flexibility-based distribution system development," *Sustainable Energy, Grids and Networks*, vol. 30, p. 100594, Jun. 2022.

[3] "Directive (EU) 2019/944 of the European Parliament and of the Council of 5 June 2019 on common rules for the internal market for electricity and amending Directive 2012/27/EU."

[4] M. Van Den Berg, I. Lampropoulos, and T. AlSkaif, "Impact of electric vehicles charging demand on distribution transformers in an office area and determination of flexibility potential," *Sustainable Energy, Grids and Networks*, vol. 26, p. 100452, Jun. 2021.

[5] J. Hu, H. Morais, T. Sousa, and M. Lind, "Electric vehicle fleet management in smart grids: A review of services, optimization and control aspects," *Renewable and Sustainable Energy Reviews*, vol. 56, pp. 1207–1226, Apr. 2016.

[6] P. M. S. Carvalho, L. A. F. M. Ferreira, and A. M. F. Dias, "Distribution grids of the future: Planning for flexibility to operate under growing uncertainty," *Foundations and Trends® in Electric Energy Systems*, vol. 2, no. 4, pp. 324–415, 2018.

[7] P. M. Carvalho and L. A. Ferreira, "Intrinsic limitations of load-shifting response dynamics: Preliminary results from particle hopping models of homogeneous density incompressible loads," *IET Renewable Power Generation*, vol. 13, no. 7, pp. 1190–1196, May 2019.

[8] P. M. Carvalho, J. D. Peres, L. A. Ferreira, M. D. Ilic, M. Lauer, and R. Jaddivada, "Incentive-based load shifting dynamics and aggregators response predictability," *Electric Power Systems Research*, vol. 189, p. 106744, Dec. 2020.

[9] P. M. S. Carvalho and L. A. F. M. Ferreira, "Value of Bidirectional V2G Smart Charging Responsive Services: Insights from a Simple CA Model," 2022.

[10] Z. J. Lee, T. Li, and S. H. Low, "ACN-Data: Analysis and Applications of an Open EV Charging Dataset," in *Proceedings of the Tenth ACM International Conference on Future Energy Systems*. Phoenix AZ USA: ACM, Jun. 2019, pp. 139–149.

[11] K. Nagel and M. Schreckenberg, "A cellular automaton model for freeway traffic," *Journal de Physique I*, vol. 2, no. 12, pp. 2221–2229, Dec. 1992.

[12] K. Nagel, "Particle hopping models and traffic flow theory," *Physical Review E*, vol. 53, no. 5, pp. 4655–4672, May 1996.